STUDIES ON FORMATION OF THE RADIALLY-DIRECTED ELECTRON BEAM GENERATED BY THE MAGNETRON GUN WITH A SECONDARY EMISSION CATHODE

M.I. Ayzatsky, A.N. Dovbnya, A.S. Mazmanishvili, N.G. Reshetnyak, V.P. Romas'ko,
I.A. Chertishchev
National Science Center "Kharkov Institute of Physics and Technology", Kharkov, Ukraine
E-mail: nreshetnyak@kipt.kharkov.ua

Results are reported from the experimental and model investigations of the formation of a radially-directed electron beam, which is generated by a secondary-emission cathode magnetron gun in the electron energy range between 30 and 65 keV, as the beam is transported in the decreasing magnetic field of the solenoid. The beam transport was realized in the system consisting of copper rings with an internal diameter of 66 mm; the system was at a distance of 85 mm from the magnetron gun edge. The radial beam current and its distribution along the length of the measuring ring system were investigated versus the amplitude and gradient of the magnetic field. Studies were made into the mode of electron current bunch formation. Numerical simulation data on the tubular electron flux motion in the decreasing magnetic solenoidal field are presented.

PACS: 29.27.Fh

INTRODUCTION

At present, there is a marked trend to develop and introduce commercially the beam techniques of material processing. The use of these methods provides the creation of advanced materials (metals and alloys) showing higher microhardness, corrosion- and wear-resistance, modified surfaces, etc. [1, 2]. For realization of the methods, accelerators of intense electron beams of energies between 100 and 400 keV are used [3, 4].

The NSC KIPT team has created the electron accelerator [5] based on the magnetron gun with a metal cold secondary-emission cathode. The operation of these guns relies on back bombardment of the cathode by electrons reflected back by the magnetic field, electron cloud formation in the vicinity of the cathode, and electron beam generation in crossed electric and magnetic fields. The application of the axial electron beam for irradiating flat surfaces of zirconium and the Zr1%Nb alloy has provided the nanostructured layer formation of increased hardness on the target [2]. In practical tasks with the application of electron beams, it is of importance to know the radial particle distribution as a function of the longitudinal coordinate of the magnetic system axis. One would expect the radial particle distribution to be sensitive to the magnetic field gradient as suggested in [6].

The present paper reports theoretical and experimental data from the studies on the radial electron beam formation by the secondary-emission cathode magnetron gun (SECMG) during the beam transport in the decreasing magnetic field of the solenoid. The feasibility of inner tubular surface irradiation has been investigated.

EXPERIMENTAL SETUP AND RESEARCH PROCEDURES

Experiments were performed on the electron accelerator to investigate the formation of a radial electron beam generated by the SECMG, as well as to measure the beam parameters during its transport in the decreasing magnetic field of the solenoid. The schematic diagram of the setup is presented in Fig. 1.
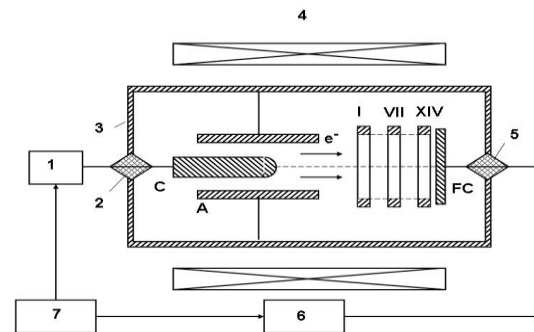
Fig. 1. Schematic of the experimental setup:
1 – high-voltage pulse generator, magnetron gun with the secondary-emission cathode C and anode A;
2, 5 – insulators; 3 – vacuum chamber; 4 – solenoid;
6 – computer measuring system; 7 – synchronizer;
FC – Faraday cup; I – XIV – metal rings

For energizing the magnetron gun, a pulse generator (1) was used, which provided voltage pulses with a spike of ~ 150 kV, pulse plateau amplitude ~ 100 kV, pulse length ~ 15 μs. The electron source (C – cathode, A – anode) is located in the vacuum volume (3). For electron beam generation, a magnetron gun, with the Ø78 mm anode and the Ø36 mm cathode, was used. The magnetic field for electron beam generation and transport is created by the solenoid (4) consisting of 4 coils, which are energized by dc sources. By varying the current in each of the coils, it is possible to change the amplitude and longitudinal distribution of the magnetic field along the axis of the magnetron gun and the beam transport channel. The observed data on the parameters of voltage pulses, the currents in radial and axial directions were processed by means of a computer measuring system (6).

The measuring system, intended for investigating radial current distributions, consists of 14 copper rings with an inner diameter of 63 mm, and of width 8 mm. The rings are spaced at intervals of ~1.5 mm, being insulated from each other and from the earth. Behind the 14th ring, there is the Faraday cup, which serves to measure the current in the axial direction.

11

The measuring system is located in the magnetic field created by the solenoid. Besides, to provide a local change in the rate of the solenoidal field decrease, a stray magnetic field created by annular SmCo$_5$ magnets is used. The magnets are placed along the axis of the system, behind the Faraday cup. The measurement of the stray magnetic field of the annular magnet versus the beam transport channel length z has shown the field to be sharply nonuniform, viz., it decreases by a factor of 2.5 at a distance of 12 mm from the magnet assembly surface, and then degrades in a smooth manner.

EXPERIMENTAL RESULTS AND DISCUSSION

Electron beam size measurements were performed along the axis of the system during beam transport in both the uniform and decreasing magnetic fields at energies ranging between 75 and 85 keV.
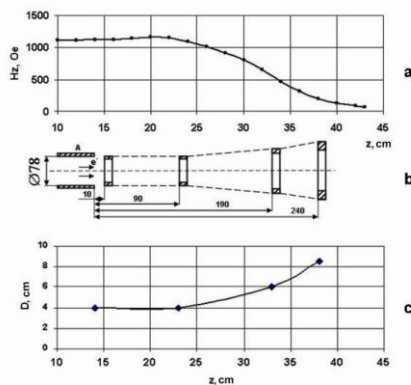

Fig. 2. Magnetic field distribution along the axis of the system (a), geometric characteristics of the beam at different distances from the anode edge of the magnetron gun (b), and the outside beam diameter versus transport length z (c)

Fig. 2 shows the magnetic field distribution along the axis of the system (a), and also, the inside and outside diameters of the beam (b) at different distances from the magnetron gun anode. The transverse beam dimensions were determined using the imprints obtained on the aluminum targets. As is seen from Fig. 2, after the anode edge, the magnetron gun forms a tubular electron beam with the O.D. ~ 40 mm and the wall thickness equal to ~ 2 mm. From Fig. 2,c, it can be seen that at the beam transport in a uniform magnetic field (~1100 Oe) for a distance of 90 mm from the magnetron gun edge, the beam diameter remained practically the same.

The magnetic field decrease down to ~ 500 Oe at distances of 190 (at ~ 500 Oe) and 240 mm (~200 Oe) from the gun edge led to the increase in the outside diameters of up to 60 and 85 mm, respectively. Besides, with the magnetic field decrease the beam cross-section thickness also increases.

Fig. 3,a shows the beam imprint obtained at a distance of ~190 mm from the anode edge of the magnetron gun, and Fig. 3, gives the electron density distribution (relative units) in the diameter in the horizontal plane, resulting from the treatment of the digital file. As is seen from Fig. 3,a, the beam has a ring form with a uniform azimuthal intensity distribution, while Fig. 3,b shows that the amplitudes of darkening on the diametri-

cally opposite edges of the imprint are practically the same.
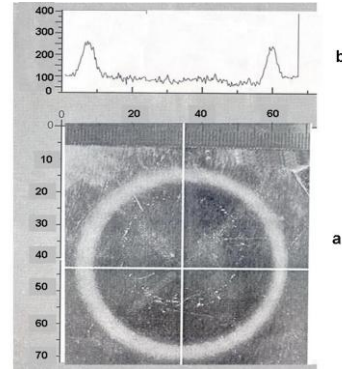

Fig. 3. Beam imprint on the aluminum target (a) and the electron density distribution in the diameter in the horizontal plane (b)

Experiments were carried out to investigate the formation of a radially-directed electron beam generated by a secondary-emission cathode magnetron gun, as well as to measure the beam parameters, as the beam is transported in the decreasing magnetic field of the solenoid in the energy range between 30 and 65 keV.

Typical oscillograms of current pulses in the radial direction ($I_9…I_{14}$), taken from 6 rings (9-14) of the measuring system, and also, of the cathode voltage pulse (U) are shown in Fig. 5. The data were obtained at the magnetic field distribution shown in Fig. 4 (curve 3).
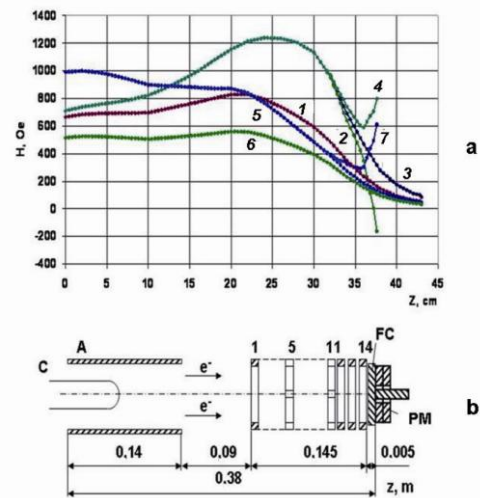

Fig. 4. Longitudinal magnetic field distribution along the magnetron gun axis and the beam transport channel (curves 1-4) (a); layout of gun elements and the radial beam current measuring system (b).
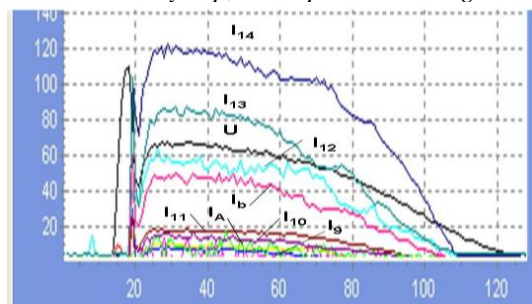A – anode; C – cathode, 1-14 – metal rings; FC – Faraday cup; PM – permanent magnets

Fig. 5. Oscillograms of radial currents ($I_{14}…I_9$) taken from rings (9-14) and the cathode voltage pulse (U)

Fig. 6 shows histograms of radial current distribution on the rings at the magnetic field distribution shown in Fig. 4 (curves 3, 5).

With the given magnetic field distribution (Fig. 4, curve 5), as is obvious from Fig. 6(1), the highest radially-directed current was registered on the 11th ring, making ~ 35% of the beam current. The magnetic field in the location area of the 11th ring was decreasing with the field gradient of ~ 70 Oe/cm at a magnetic field strength of ~ 300 Oe in the middle of the ring.

The studies have revealed the possibility to control the current in the radial direction and the current distribution along the rings of the measuring system by varying the distribution and amplitude of the magnetic field along the beam transport axis. It has been found that at the given magnetic field distribution (see Fig. 4, curve 3), the maximum radial current was registered (see Fig. 6(2)) on the 14th ring, making ~ 40% of the beam current. In this case, the radial current to the 11th ring decreased by a factor of 3.5. The current in the radial direction was registered from the 14th to the 9th ring. The magnetic field in the location area of the 11th ring was decreasing with the field gradient of ~ 100 Oe/cm at a magnetic field strength of ~ 350 Oe in the middle of the ring.
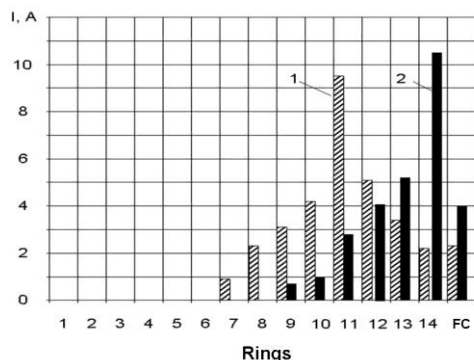

Fig. 6. Comparative histogram of ring currents for different magnetic field distributions: 1 – magnetic field (see Fig. 4, curve 5); 2 – magnetic field (see Fig. 4, curve 3)

In the performance of the experiments, electron current bunches were formed in radial and axial directions at the magnetic field distribution shown in Fig. 4, curve 6, and at voltage of 31 kV. The bunch formation took place when the longitudinal magnetic field near the lower boundary of electron beam formation exceeded the Hell cutoff field by factors of 1.1 to 1.2 [7]. As can be seen from the obtained oscillograms (Fig. 7) showing voltage (U) and current ($I_9…I_{14}$) pulses in radial and axial (I_b) directions, two characteristic regions can be distinguished. The first region characterizes the oscillation mode of radial/axial currents, and the second region represents the customary mode of beam formation.

It is apparent from Fig. 7 that the current in the radial direction and to the Faraday cup appears as a sequence of bunches, the amplitude and shape of each bunch being, in this case, practically coincident. The appearance of azimuthal current distribution of each bunch remains unchanged. This indicates that the processes of electron cloud formation of each bunch occur in a similar way. As concerns the bunches themselves, they all show rather high amplitude stability and azimuthal homogeneity.

With voltage amplitude decrease at the pulse peak due to the discharge of the storage capacitor in the pulse generator circuit, the gun operates in the customary regime of current forming. This is evident in the oscillograms (see Fig. 7) taken after the end of the oscillatory process.

Experiments were performed, where the main field of the solenoid was supplemented with an additional scattered field, which was created by annular magnets. The studies were carried out for two cases: (i) directions of the magnetic fields of the annular magnets and of the solenoid were opposite (see Fig. 4); and (ii) the fields of the annular magnets and solenoid coincided in the direction (see Fig. 4, curves 4 and 7).
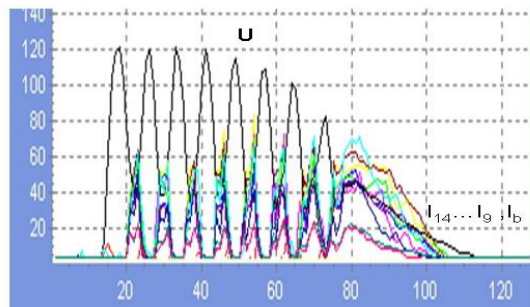

Fig. 7. Oscillograms of radial currents ($I_{14}…I_9$), axial current (I_b) and the cathode voltage pulse (U)

The experiments carried out at a cathode voltage ranging between 30 and 65 keV have shown that the radial current value and its distribution along the metal ring length are dependent on the amplitude and distribution of the magnetic field along the axis of the system, the field decrease gradient and the direction of the solenoid field.

Fig. 8 shows typical oscillograms of cathode voltage pulses (U) and radial currents (I_{13}, I_{14}) taken from rings 13 and 14 at the magnetic field distribution given in Fig. 4, curve 2.
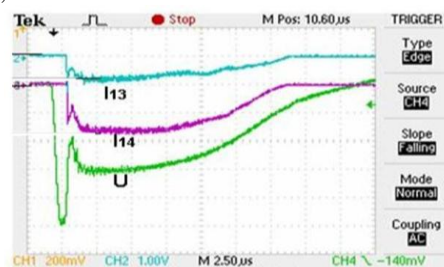

Fig. 8. Oscillograms of radial currents (I_{13}, I_{14}) and the cathode voltage pulse (U):
I_{13} – 5 A/div, I_{14} – 14 A/div, U ~ 15 kV/div

In the experiments, it has been established that at the given magnetic field distribution (Fig. 9(3)), the radial current to the 14th ring makes ~ 70% of the beam current at an electron energy of ~ 41 keV. The magnetic field in the location area of the 14th ring had the field decrease gradient of ~ 280 Oe/cm. The radial current to the 13th ring and the 12th ring was measured to be ~ 19 and 4%, respectively, while the axial current was determined to be ~ 10% of the beam current.

The investigations have demonstrated that with reduction in the magnetic field gradient down to ~ 100 Oe/cm (i.e., without an additional magnetic field) in the region of the 14th ring (see Fig. 4, curve 5), the

13

current in the radial direction to the ring decreased by a factor of 2.1 (see Fig. 9(2)) as compared with the case of using an additional magnetic field (see Fig. 4, curve 2). In this case, the radial currents to the rings from N 13 to N 10 correspondingly increased.
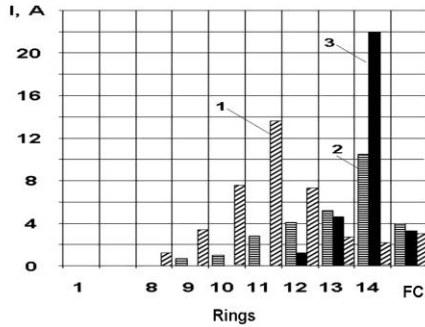

Fig. 9. Comparative histogram of ring currents for different magnetic field distributions: 1 – magnetic field (see Fig. 4, curve 1); 2 – magnetic field (see Fig. 4, curve 3); 3 – magnetic field (see Fig. 4, curve 2)

By varying the magnetic field amplitude and distribution along the axis of the magnetron gun and the beam transport channel (see Fig. 4, curve 1), it was possible to regulate the radial current along the length of the measuring ring system. As can be seen from Fig. 4, curve 1, in the cathode and anode regions, and then, along the whole measuring system, too, the field was decreasing. At that magnetic field distribution (see Fig. 9(1)), the peak current drifted to the 11th ring and came up to ~ 35% of the beam current at a cathode voltage of 48 kV. In the region of the 11th ring, the magnetic field was decreasing with the field gradient of ~ 70 Oe/cm. Since the 11th ring was cut into four identical segments, then by taking radial current readings from two opposite, separated by 180°, segments one may judge about the azimuthal beam uniformity.

Fig. 10 gives the oscillograms of radial current pulses taken from the 2nd and 4th segments of the 11th ring. It is apparent from the oscillograms that the shape and amplitude of signals from the segments, obtained at the magnetic field distribution shown in Fig. 4, curve 1, are practically coincident. The coefficient of azimuthal beam nonuniformity was found to be ~ 1.1 (Fig. 11).
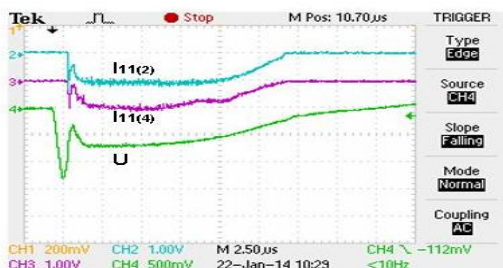

Fig. 10. Oscillograms of current pulses in the radial direction from two segments of the 11th ring and the cathode voltage pulse (U): $I_{11(2)}$ – 3.6 A/div, $I_{11(4)}$ – 3.5 A/div, U~30 kV/div

So, the present investigations have shown that the optimization in the distribution of both the magnetic field created by the solenoid and annular magnets, and the field decrease gradient, increases the portion of electrons falling on one ring up to 70%.
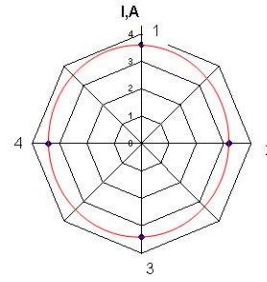

Fig. 11. Azimuthal nonuniformity of radial beam current distribution on the 11th ring

Fig. 12 illustrates the current to the 14th ring as a function of the cathode voltage in the range between 30 and 60 kV.
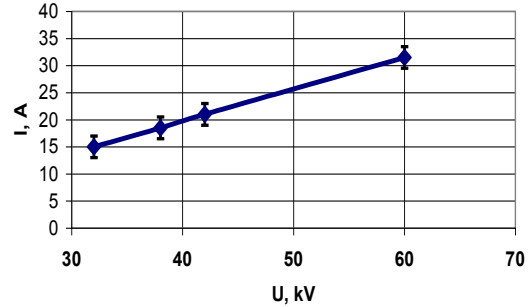

Fig. 12. Radial current to the 14th ring versus cathode voltage

By varying the magnetic field amplitude and distribution, it was possible to regulate the current in the radial direction along the measuring system length, and hence, the place of electron irradiation.

Experiments were performed, where the total magnetic field showed a spike (see Fig. 4, curves 4,7) (the field directions of the annular magnets and of the solenoid were coincident). In this case, the radial current distributions substantially differ from the distributions obtained in the case the decreasing magnetic field (see Fig. 4, curve 2).
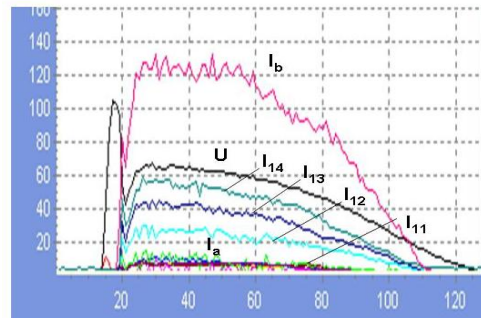

Fig. 13. Distribution of currents ($I_{11}...I_{14}$) in radial and axial directions (I_b) on the rings (11-14), and the cathode voltage distribution (U)

Typical oscillograms of radial current pulses (($I_{11}...I_{14}$) taken from four rings (11-14) of the measuring system, and also, the axially-directed current I_b, as well as the cathode voltage pulse (U) are shown in Fig. 13. The results were obtained at the magnetic field distribution shown in Fig. 4, curve 7. It is evident from the given oscillograms of radial and axial currents that the pulse forms coincide with each other throughout the duration of the cathode voltage pulse.

Fig. 14 gives the histograms of radial and axial currents on the rings, which were obtained at the magnetic

field distribution presented in Fig. 4, curves 4, 7. As is seen from Fig. 14 (1), at the magnetic field distribution shown in Fig. 4, curve 7, the peak current in the radial direction was registered on the 14th ring, making ~ 33% of the beam current, whereas the current in the axial direction was ~ 60% at the cathode voltage ~ 41 kV.
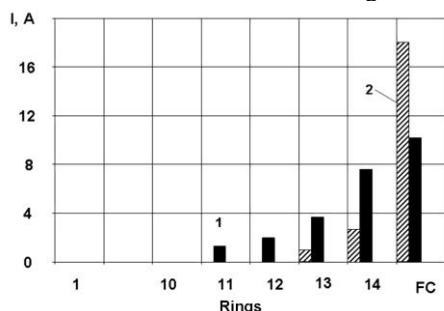

Fig. 14. Comparative histogram of currents in both radial and axial directions for two magnetic field distributions: 1 – magnetic field (see Fig. 4, curve 7); 2 – magnetic field (see Fig. 4, curve 4)

The magnetic field in the region of the 14th ring amounted to 500 Oe with the gradient of the field increase ~ 220 Oe/cm. As it is seen from Fig. 14(2), the variation of the magnetic field amplitude and distribution along the magnetic gun axis and the beam transport channel (see Fig. 4, curve 4) has led to a nearly 3-fold reduction in the radial current to the 14th ring. In this case, the current in the axial direction increased up to ~ 80% of the beam current, as compared to the current obtained at the magnetic field distribution shown in Fig. 4, curve 7. The magnetic field in the region of the 14th ring was 730 Oe with the field increase gradient ~ 150 Oe/cm.

Numerical simulation has been made to inquire into the dynamics of the electron beam in the decreasing magnetic field of the solenoid (see Fig. 4 to curve 4). The developed software makes use of the Monte-Carlo method and the Runge-Kutta procedure, the application of which has been described in [8]. Below we give the dependences obtained for the case of the magnetic Fig. 4, curve 3.
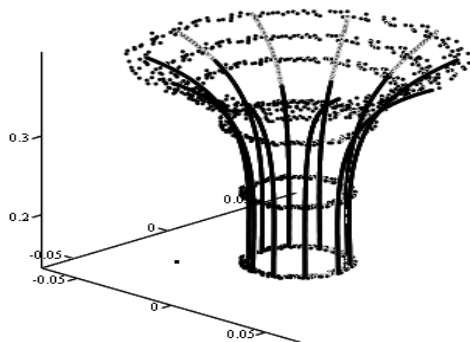

Fig. 15. Beam profile is shown by vertical beam cross-sections; the sample size is 200 particles; the coordinates are given in meters, z axis is vertical

Fig. 15 shows the trajectories of 10 particles uniformly distributed at emission in the azimuth (with the $2\pi/10$ step) along with the vertical beam cross-sections. In the radial direction, the beam, composed of 200 emitted particles, was specified by means of a uniform distribution density on the cathode ring with the inner radi-

us r_a and the outer radius r_b. The computation was carried out within the interval $r_a \le r \le r_b$ at $r_a = 18$ mm and $r_b = 22$ mm. It is apparent from Fig. 15 that the beam profile corresponds to the magnetic field distribution along the axis of the system at different distances from the anode edge of the magnetron gun (see Fig. 2, curve 2). In this case, as the magnetic field decreases, the particle radius increases.

In numerical simulation, we have used azimuthal homogeneity of emitted particle distribution. On this account, the beam cross-sections for different vertical coordinate z values remain homogeneous in azimuth. Fig. 16 shows the corresponding cross-sections. Note that in view of the axial directivity of the magnetic field (see Fig. 2) the cross-sections for the distances $z = 0.15$ and 0.23 m are practically coincident, and the points in the figure that correspond to the particles considered are overlapping.
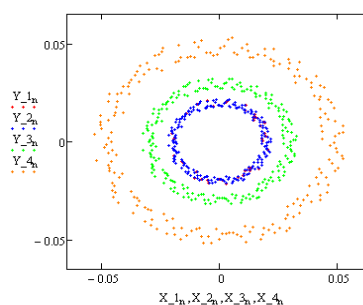

Fig. 16. Beam cross-sections for different vertical coordinate values $z = 0.15$ m (red points), 0.2 3 m (blue), 0.33 m (green) and 0.38 m (orange)

So, the beam particles have laminar motion. In this case, the distributions of emitted electrons from the start successively transform into corresponding distributions in each of the particle coordinates for the chosen axial coordinates z. Fig. 17 shows a set of histograms of r-coordinate values for the sample of volume N=1000 particles. The emitting particles were assigned to be in the radial direction by means of a homogeneous distribution density within the interval $r_a \le r \le r_b$ at $r_a = 18$ mm and $r_b = 19$ mm. Histograms of X- or Y-coordinates have a similar appearance for the same z-values in the beam transport channel.

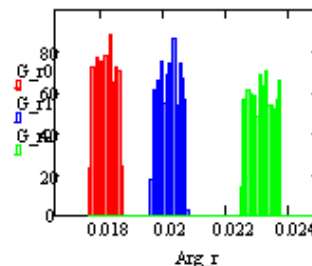*Fig. 17. Histograms of beam particle r-coordinates at $z = 0.14$, 0.30 and 0.37 m (sample size N=1000 particles)*

The simulation data suggest the conclusion that the assumed model of motion and the chosen initial conditions for the beam particles provide a way of obtaining the dependences, the behavior of which is in good agreement with the given experimental data.

CONCLUSIONS

The present studies have demonstrated the possibility to form a stable radial electron beam during its transport in the decreasing magnetic field of the solenoid. It has been found experimentally that the radial current value and the current distribution along the transport axis are dependent on the magnetic field distribution along the axis of the system and the field decrease gradient. It has been demonstrated that by regulating the magnetic field distribution it is possible to attain a 70% incidence of electrons on the desired ring. By varying the magnetic field amplitude and the field distribution on the cathode one can form separate bunches of radial/axial currents. The mathematical modeling of the electron flow dynamics has resulted in the dependences that are in good agreement with the measured data.

In the subsequent studies, when solving the problems of modifying the inner surfaces of tubular items, it would be necessary to increase the energy density on the samples at the expense of increasing the electron energy in the range between 100 and 120 keV, and also, to choose the optimum characteristics of electron irradiation.

REFERENCES

1. M.F. Vorogushin, V.A. Glukhikh, G.Sh. Manukyan, D.A. Karpov, M.P. Svin'yin, V.I. Ehngel'ko, B.P. Yatsenko. Beam and ion-plasma technologies // *Problems of Atomic Science and Technology. Series "Physics of Radiation Effects and Radiation Materials Science"*. 2002, № 3, p. 101-109.
2. A.N. Dovbnya, S.D. Lavrinenko, V.V. Zakutin, et al. Surface modification of zirconium and Zr1%Nb alloy by the electron beam of the magnetron gun-based accelerator // *Problems of Atomic Science and Technology. Series "Physics of Radiation Effects and Radiation Materials Science"*. 2011, № 2, p. 39-45.
3. V. Engelko, G. Mueller, A. Andreev, et al. Pulsed Electron Beam Facilities (GESA) for Surface Treatment // *Proc. of the 10th International Conf. on Applied Charged Particle Accelerators in Medicine and Industry*. St.-Petersburg, Russia. 2001, p. 412-4172.
4. O.V. Garkusha, S.P. Maslennikov, A.E. Novozhilov, Eh.Ya. Shkol'nikov. A high-current accelerator of microsecond electrons for radiation-technological purposes // *Proc. of the XI International Meeting on the Use of Charged Particle Accelerators in Industry and Medicine*. St. Petersburg, Russia. 2005, p. 126.
5. A.N. Dovbnya, V.V. Zakutin, N.G. Rashetnyak, et al. Studies of beam formation in the electron accelerator with a secondary-emission source // *Visnyk KhNU. Series "Nuclei, Particles, Fields"*. 2006, № 732, 2(30), p. 96-100.
6. A.N. Dovbnya, N.S. Repalov, Yu.D. Tur. Defocusing of a modulated electron flow in the region of longitudinal magnetic field decrease // *Problems of Atomic Science and Technology. Series "Technique of Physical Experiment"*. 1984, iss. 2(19), p. 1-80.
7. N.I. Aizatsky, A.N. Dovbnya, V.V. Zakutin, et al. Electron current bunch formation in the magnetron gun with a secondary-emission cathode // *Journal of Kharkiv National University. Physical series "Nuclei, Particles, Fields"*. 2008, №794, iss. 1(37), p. 85-89.
8. N.I. Aizatsky, V.N. Boriskin, A.N. Dovbnya, et al. Radial electron beam formation by the magnetron gun with a secondary-emission cathode: experiment and theory // *Applied Radioelectronics*. 2014, v. 13, № 2, p. 127-34.

ИССЛЕДОВАНИЕ ФОРМИРОВАНИЯ ЭЛЕКТРОННОГО ПУЧКА В РАДИАЛЬНОМ НАПРАВЛЕНИИ, ГЕНЕРИРУЕМОГО МАГНЕТРОННОЙ ПУШКОЙ С ВТОРИЧНО-ЭМИССИОННЫМ КАТОДОМ

Н.И. Айзацкий, А.Н. Довбня, А.С. Мазманишвили, Н.Г. Решетняк, В.П. Ромасько, И.А. Чертищев

Приведены результаты исследований и моделирования по формированию электронного пучка в радиальном направлении магнетронной пушкой с вторично-эмиссионным катодом в диапазоне энергий электронов 30…65 кэВ при транспортировке его в спадающем магнитном поле соленоида. Транспортировка пучка осуществлялась в системе, состоящей из медных колец с внутренним диаметром 66 мм, находящейся на расстоянии 85 мм от среза магнетронной пушки. Изучена зависимость тока пучка в радиальном направлении и его распределение вдоль длины колец измерительной системы от амплитуды магнитного поля и градиента спада поля. Исследован режим формирования сгустков электронного тока. Приводятся результаты численного моделирования по движению трубчатого электронного потока в спадающем магнитном поле соленоида.

ДОСЛІДЖЕННЯ ФОРМУВАННЯ ЕЛЕКТРОННОГО ПУЧКА В РАДІАЛЬНОМУ НАПРЯМКУ, ЩО ГЕНЕРУЄТЬСЯ МАГНЕТРОННОЮ ГАРМАТОЮ З ВТОРИННО-ЕМІСІЙНИМ КАТОДОМ

М.І. Айзацький, А.М. Довбня, О.С. Мазманішвілі, М.Г. Решетняк, В.П. Ромасько, І.О. Чертіщев

Приведено результати досліджень і моделювання по формуванню електронного пучка в радіальному напрямку магнетронноюгарматою з вторинно-емісійнимкатодом у діапазоні енергій електронів 30…65 кеВ при транспортуванні його в спадаючому магнітному полі соленоїда. Транспортування пучка здійснювалося в системі, що складається з мідних кілець з внутрішнім діаметром 66 мм, що знаходиться на відстані 85 мм від зрізу магнетронної гармати. Вивчена залежність у радіальному напрямку струмупучка і його розподіл уздовжкілець вимірювальної системи від амплітуди магнітного поля і градієнта спаду поля. Досліджено режим формування згустків електронного струму. Наведено результати чисельного моделювання за рухом трубчастого електронного потоку в спадаючому магнітному полі соленоїда.